Received: 22 February 2021 | Revised: 16 July 2021 | Accepted: 29 July 2021

DOI: 10.1111/ejn.15419

RESEARCH REPORT

EJN European Journal of Neuroscience FENS WILEY

The missing N1 or jittered P2: Electrophysiological correlates of pattern glare in the time and frequency domain

Austyn J. Tempesta[1] | **Claire E. Miller**[1] | **Vladimir Litvak**[2] | **Howard Bowman**[1,3] | **Andrew J. Schofield**[1,4]

[1]School of Psychology, College of Life and Environmental Sciences, University of Birmingham, Edgbaston, Birmingham, UK

[2]Wellcome Centre for Human Neuroimaging, University College London, London, UK

[3]School of Computing, University of Kent, Canterbury, UK

[4]School of Psychology, College of Health and Life Sciences, Aston University, Birmingham, UK

Correspondence
Howard Bowman, School of Psychology, College of Life and Environmental Sciences, University of Birmingham, Edgbaston, Birmingham, B15 2TT, UK.
Email: h.bowman@bham.ac.uk

Abstract

Excessive sensitivity to certain visual stimuli (cortical hyperexcitability) is associated with a number of neurological disorders including migraine, epilepsy, multiple sclerosis, autism and possibly dyslexia. Others show disruptive sensitivity to visual stimuli with no other obvious pathology or symptom profile (visual stress) which can extend to discomfort and nausea. We used event-related potentials (ERPs) to explore the neural correlates of visual stress and headache proneness. We analysed ERPs in response to thick (0.37 cycles per degree [c/deg]), medium (3 c/deg) and thin (12 c/deg) gratings, using mass univariate analysis, considering three factors in the general population: headache proneness, visual stress and discomfort. We found relationships between ERP features and the headache and discomfort factors. Stimulus main effects were driven by the medium stimulus regardless of participant characteristics. Participants with high discomfort ratings had larger P1 components for the initial presentation of medium stimuli, suggesting initial cortical hyperexcitability that is later suppressed. The participants with high headache ratings showed atypical N1-P2 components for medium stripes relative to the other stimuli. This effect was present only after repeated stimulus presentation. These effects were also explored in the frequency domain, suggesting variations in intertrial theta band phase coherence. Our results suggest that discomfort and headache in response to striped stimuli are related to different neural processes;

List of Abbreviations: ADHD, Attention Deficit Hyperactivity Disorder; ANOVA, Analysis of variance; BIC, Bayesian Information Criterion; BOLD, Blood Oxygen Level Dependent; CI, Confidence Interval; CHi, Cortical hyperexcitability index; DC, Direct Current (here referring to mean level of an ERP signal after baseline correction); d.f., degrees of freedom; ERP, Event-Related Potential; EEG, Electroencephalogram; fMRI, functional Magnetic Resonance Imaging; FWE, Family-wise Error; GABA, Gamma aminobutyric acid; HGHQ, Headache and General Health Questionnaire; ICA, Independent components analysis; IHS, International headache society; MUA, Mass Univariate Analysis; NIRS, Near infrared spectroscopy; PGT, Pattern glare test; PGI, Pattern glare index; c/deg, Cycles per degree; PR-VEP, Pattern reversal visual evoked potential; ROI, Region of interest; VDS, Visual discomfort scale; VEP, Visual evoked potential; WISC-R, Wechsler intelligence scale for children (revised form).

however, more exploration is needed to determine whether the results translate to a clinical migraine population.

KEYWORDS
cortical excitability, EEG, headache, pattern glare, visual stress

1 | INTRODUCTION

Cortical hyperexcitability is a condition in which neuronal circuits in the cortex respond more strongly to stimuli than is typical or appropriate. It has been associated with many conditions including migraine (Welch et al., 1990), epilepsy (Badawy et al., 2013), multiple sclerosis (Wright et al., 2007), stroke (Beasley & Davies, 2012), autism (Kientz & Dunn, 1997) and possibly dyslexia (Kriss & Evans, 2005; Singleton & Trotter, 2005, but see also Saksida et al., 2016). People with these conditions often report enhanced sensitivity, discomfort, nausea and even pain in response to certain stimuli. In vision, high-contrast stripes with spatial frequency around 3 cycles per degree (c/deg) tend to be disruptive, and are associated with visual distortions and illusory perceptions as well as headaches (Nulty et al., 1987); and this is the basis of the pattern glare test (PGT), which is diagnostic of cortical hyperexcitability (Wilkins & Evans, 2001). For example, such stimuli are disruptive for migraine sufferers and are also triggers for those with photosensitive epilepsy (Adjamian et al., 2004; Wilkins et al., 1984). In many of the above conditions, visual distortions in text inhibit reading but can be alleviated using coloured filters (Aldrich et al., 2019; Vieira et al., 2020). Some have disrupted reading and high scores on measures of visual discomfort, cortical hyperexcitability and pattern glare (see later) but few other symptoms. Wilkins and colleagues describe such individuals as suffering from *visual stress* and posit that this condition is separate from but co-morbid with other conditions—especially where there is no obvious brain injury (Wilkins, 2003).

To pre-empt our results, we are specifically interested in the neural correlates of discomfort when viewing certain visual stimuli and headache proneness, specifically migraine, due to its links with cortical hyperexcitability. However, the overlap of symptoms noted above suggests that when comparing headache patients and control groups to assess cortical hyperexcitability, some members of the control group may have a degree of latent hyperexcitability. This possibility can be countered by recording several measures of hyperexcitability as possible covariates for analysis rather than relying on whether or not the participant is in the control or experimental group as the sole predictor of atypical neural activity. As such, we did not specifically recruit from the migraine population but rather measured headache proneness in the general population along with a range of trait and state measures for cortical hyperexcitability. Nonetheless, much of the work relating cortical hyperexcitability to headaches is in the migraine literature which we now review.

1.1 | General hyperexcitability and migraine

Migraine has been associated with the hyperexcitability of neurons in the visual cortex (Welch et al., 1990) and increased sensitivity to certain stimuli, both during and between episodes, even in the absence of a specific visual trigger (Ambrosini & Schoenen, 2006; Friedman & De Ver Dye, 2009; Spierings et al., 2001). Migraine has also been associated with atypical electroencephalogram (EEG) patterns (Marks & Ehrenberg, 1993) and an increased functional magnetic resonance imaging (fMRI) blood-oxygen level-dependent (BOLD) response to certain visual stimuli (Hougaard et al., 2014; Huang et al., 2003). These stimuli also elicit an atypical haemodynamic response function (Haigh et al., 2015; Olman et al., 2004; Vazquez & Noll, 1998).

Cortical hyperexcitability may make those with migraine and other headache disorders more sensitive to visual stimulation such as flickering lights (Wilkins et al., 1989) and striped patterns (Harle et al., 2006). Such stimuli induce visual distortions and eyestrain and are also trigger stimuli for some individuals (Wilkins, 1986, 1995; Wilkins et al., 1979, 1980). Flickering light sources up to around 100 Hz are problematic, and those working under flickering fluorescent lighting experience more headaches and other symptoms than those working in natural light or under high-frequency fluorescent tubes (Wilkins et al., 1989). Of greater interest here are the visual distortions and discomfort resulting from striped stimuli. Many individuals see distortions when viewing high-contrast square wave gratings (stripes), and this tendency increases somewhat with spatial frequency. However, those who suffer visual stress, including migraineurs, tend to see more distortions when viewing midrange spatial frequencies around 3 c/deg (Harle

et al., 2006), such that the difference in the number of distortions seen between 3 and 12 c/deg patterns is seen as diagnostic of visual stress (Evans & Stevenson, 2008). This comparison is the basis for the PGT developed by Wilkins and Evans (2001). Although Wilkins et al. (2016) advocate using only the midfrequency grating in clinical settings where reproduction quality and viewing distance accuracy make use of the high-frequency pattern problematic, here we had good control over the stimulus and viewing conditions and presented the high-frequency grating with accuracy. We thus prefer the original comparison of stimuli although we make a comparison of discomfort ratings rather than the number of observed distortions.

1.2 | EEG findings

If cortical hyperexcitability is responsible for heightened sensitivity to simple visual patterns, we might expect to find increased neural activity associated with early visual processing in response to such patterns. A few early studies measured ERPs in response to non-patterned flashes of light, finding these have greater amplitude than patterned flashes in the early components of the ERP waveform (Brinciotti et al., 1986; Connolly et al., 1982; Lehtonen, 1974; MacLean et al., 1975, but see also Richey et al., 1966). However, EEG studies have more typically measured pattern-reversal visual evoked potentials (PR-VEPs) in response to chequerboard stimuli and have provided mixed results for the amplitude and latency of early visual components: Some studies show increased amplitude and latency and others found a reduction; however, most found that PR-VEPs in migraine were similar to those in controls (see Ambrosini & Schoenen, 2006, for a review). The evidence for habituation abnormalities is more consistent, suggesting that those with migraine fail to habituate to repeated stimulation with the same stimulus (Afra et al., 1998; Coppola et al., 2009; Schoenen et al., 1995; Wang et al., 1999). EEG waveforms also vary with migraine phase, paradoxically being closer to that of typical non-sufferers just prior to migraine onset (Shahaf, 2016), which may explain the somewhat contradictory results for PR-VEP amplitudes. The common use of non-patterned flashes and chequerboard stimuli to test VEP responses in migraine may be suboptimal since stripes of a midrange frequency, rather than cheques, are thought to be more aggravating for migraine sufferers and others with visual stress or pattern glare symptoms (Wilkins, 1995). It is possible then that VEP studies have not explored the strongest or most pertinent EEG responses in this population.

Few studies have recorded brain activation in response to pattern glare stimuli. Huang et al. (2003) applied such stimuli to a migraine population showing increased fMRI activity in the occipital cortex, consistent with the cortical hyperexcitability theory in migraine. To our knowledge, only two studies have previously measured ERPs in a headache prone population using pattern glare like stimuli. Fong et al. (2020) found differences between migraine sufferers and controls at around 200- and 400-ms poststimulus onset. Their migraine group showed greater negativity at 200 ms for high-frequency gratings (13 c/deg). Indeed, their main findings were on the high-frequency grating, while in contrast, the findings we report here occur with the clinically relevant, medium-frequency grating (3 c/deg). Haigh et al. (2019) found larger amplitude N1 and N2 ERP components in a migraine group viewing chromatic gratings. These enlarged responses were associated with higher discomfort ratings when viewing the stimuli.

1.3 | BOLD and NIRS findings

Cortical hyperexcitability has also been observed in the fMRI BOLD responses of those who have heightened sensitivity to striped patterns. Elevated BOLD signals have been found in primary (striate) visual cortex as well as extra-striate visual cortex, pre-cortical structures and areas of the frontal cortex (See Schwedt et al., 2015, for a review). In one study, heightened BOLD responses to striped stimuli in cortical area V3 were found to reduce when the migraine patients wore glasses with a prescribed colour tint versus a similar tint or grey filters (Huang et al., 2011). Indeed, similar coloured filters have been found to reduce distortions on the PGT (Harle et al., 2006).

Studies using near infrared spectroscopy (NIRS) have found evidence that patients with migraine have shorter oxyhaemoglobin responses than healthy controls (Coutts et al., 2012). This result is in line with other findings suggesting that patients with lower concentrations of GABA produce higher amplitude but shorter, BOLD responses in the visual cortex (Muthukumaraswamy et al., 2012). The result also supports the hypothesis that GABAergic mechanisms affect local cortical excitability (Semyanov et al., 2003), although the glutamatergic system seems to be the primary focus for hyperexcitability in migraine. Haigh et al. (2015) explored the link between pattern glare and the haemodynamic response in the general population, comparing stimuli known to be aggravating in migraine with those that are not. The amplitude of the haemodynamic response was largest for stripes with high chromatic contrast, these being more aggravating.

Moving striped stimuli showed a steeper decline in the haemodynamic response at stimulus offset compared with static gratings. This result suggests that, even in the general population, the shape of the haemodynamic response appears to reflect stimulus potency: The stimuli that evoke the most discomfort in migraine produce the largest amplitude and the steepest slope in oxyhaemoglobin and deoxyhaemoglobin responses in the general population.

1.4 | Trait-dependent measures

The neurophysiological tests described above tend to be costly and difficult to administer as a diagnostic test. The PGT is an easy to use clinical tool, but like some of the physiological measures, it may be state dependent—varying from day to day, specifically with migraine phase (Wilkins et al., 1984). Such state measures are useful for judging if an individual is suffering from visual hypersensitivity at a particular moment in time but may be poor measures of their general tendency to suffer hyperperception. Hypersensitivity results in distortions of the visual image, which can be disruptive for everyday tasks such as reading and can cause discomfort in everyday environments. Based on these and other symptoms, Conlon and colleagues developed a 23-item questionnaire (Visual Discomfort Scale—VDS; Conlon et al., 1999) for which scores correlate positively with headache severity and visual distortions when viewing square wave gratings (similar to the pattern glare stimuli) and letter stimuli and negatively with reading speed and performance on the digit symbol subtest from the revised Wechsler Intelligence Scale for Children (WISC-R). In an attempt to address cortical hyperexcitability more broadly, if still indirectly, Braithwaite et al. (2015) developed the Cortical Hyperexcitability index (CHi), a 27-item questionnaire in which symptoms are rated for both intensity and frequency of occurrence, although these scores can be merged. Both the VDS and CHi can be regarded as trait measures of cortical hyperexcitability in that they measure the proneness of the participant to episodes of hyperexcitability based on their previous experience.

1.5 | Overview

In this study, participants were not selected based on their migraine or headache status; rather ERP and EEG results were correlated with scores on a range of headache and hyperexcitation measures within a single group drawn from the general population. We measured EEG responses to visual stimuli based on those used in the PGT in a novel paradigm where stimuli were repeated (turned on and off but not phase reversed) at a low temporal frequency allowing the recording of both ERPs and the consideration of repetition/habituation effects. Thus, we compared stimuli known to be aggravating in migraine with those that are less aggravating, in a paradigm that allows the separation of initial and habituated responses. State measures of discomfort in response to the PGT stimuli were also taken. We hypothesised that symptoms of headache, visual discomfort, cortical hyperexcitability and pattern glare would correlate with increased amplitude and atypical timing of early ERP components at occipital electrodes and that this would manifest in part as differential responses to repeated stimulation.

Recent discussion of how to improve the reliability of statistical procedures in psychology and cognitive neuroscience research has suggested that authors should explicitly justify their choice of alpha level (Lakens et al., 2018). Additionally, it has been argued that *p*-values around 0.05 do not correspond to strong evidence to reject the null. This has been done through comparisons to Bayes factors calculated on the same data (Wetzels et al., 2011). However, importantly, while our alpha level for family-wise error (FWE) correction is at the classic 0.05 level, this is applied over voxel level *t*-values and these are much more extreme in our statistically significant clusters. Specifically, whether correcting at the peak or cluster level, the (time–space) voxels that we report as statistically significant all have *p*-values that are 0.001 or smaller. The analysis performed in Wetzels et al. (2011) suggests that a *p*-value less than 0.001 always provides at least strong, and almost always very strong or decisive, evidence for the alternative under a Bayesian analysis. Additionally, if one were to apply a Bayesian analysis to neuroimaging data, the FWE correction would not be applied (Friston et al., 2002; Friston & Penny, 2003). Consequently, although Bayesian mass-univariate analyses are not typical in neuroimaging, from a Bayesian perspective, the effects we report would be expected to correspond to very strong or even decisive evidence to reject the null. In this sense, our choice of statistical thresholds is more conservative than it may at first seem.

2 | MATERIALS AND METHODS

2.1 | Participants

Forty undergraduate and postgraduate students, recruited at the University of Birmingham, gave their informed consent and were compensated with £24 for participating.

Participants with a history of psychiatric, psychological and neurological conditions or a history of unconsciousness, convulsions or epilepsy were excluded from the study. One participant chose to leave the experiment, one was removed due to an equipment malfunction, one due to an artefact that could not be removed and three were removed during data pre-processing due to a lack of usable trials (fewer than 20% per condition). There were thus 34 usable datasets (male = 13, female = 21, mean age = 22.5 y, range = 18–32 years, standard deviation = 2.86). This study was approved by The Science Technology Engineering and Maths Ethics Committee at the University of Birmingham in adherence with The 2008 Declaration of Helsinki.

2.2 | Stimuli, equipment and measures

We used stimuli similar to those used in the PGT (Wilkins & Evans, 2001). Stimuli comprised horizontal square-wave gratings (contrast = 75%) at three different spatial frequencies (0.37, 3 and 12 c/deg: described as thick, medium and thin, respectively; see Figure 1) displayed in a circular window with diameter 15.2 deg (23 cm, 732 pixels, at a viewing distance of 86 cm). These stimuli were created in MATLAB using the Psychophysics Toolbox (Brainard, 1997; Kleiner et al., 2007; Pelli, 1997) and displayed on a 60-Hz Samsung 932BF LCD monitor (Samsung Electronics, Suwon, South Korea) with pixel pitch 0.02 deg/pixel. Each cycle of the 12 c/deg grating occupied 4 screen pixels; 3 c/deg, 16 pixels and 0.37 c/deg, 130 pixels, respectively, such that our stimuli were represented without spatial aliasing. Stimuli were calibrated against the monitor's gamma non-linearity such that the luminance of the grey background matched the mean luminance of the gratings.

Questionnaires were used to assess participants' headache history (Headache and General Health Questionnaire, HGHQ) and tendency to suffer visual stress (CHi: Braithwaite et al., 2015; VDS: Conlon et al., 1999). We did not use the headache criteria specified by the International Headache Society (IHS, 2018) to diagnose migraine. These are criteria for clinical diagnosis and do not provide scale measures of headache proneness. However, the criteria rely heavily on headache intensity, nature, duration and frequency and the presence of aura, all of which were recorded by the HGHQ. EEG recordings were made using a 128-channel BioSemi (University of Amsterdam) EEG system in a dark, quiet room.

2.3 | Procedure

After the EEG electrodes had been applied, participants began the experiment with a 5-min resting period and then were presented with three blocks, each containing six trials for each of the three stimuli. Thus, each participant observed 18 trials per stimulus type. Each trial contained between seven and nine presentations (termed here onsets) of the same stimulus each lasting 3 s followed by a variable interval of 1–1.4 s. The stimuli, which were static and did not flicker, did not vary in any way between presentations within a trial. Thus, trials lasted between 28 and 39 s depending on the number of stimulus repeats and the duration of the blank intervals. Overall then, participants received considerable exposure to potentially aggravating stimuli and trial counts were kept low to minimise the potential harm from such exposure at the risk of low epoch counts for individual onsets. We later averaged across Onsets 2–8 (that is the second through eighth onsets within the longer trial) thus increasing the effective epochs in that analysis to 120 (Onset 8 only occurred 12 times for each condition). After each trial, the participant was asked to rate how comfortable they found each stimulus on a 5-point scale (1 = no discomfort, 5 = extreme discomfort) and to indicate how many onsets they saw. This additional task was designed to ensure attention to the stimuli. We assessed differences in the error rates between the three stimulus conditions, finding that the null hypothesis was moderately supported (Bayes factor for null vs. alternative, $BF_{01} = 5.81$. One-way repeated measures Bayesian ANOVA with BIC method in SPSS, IBM, NY). Due to

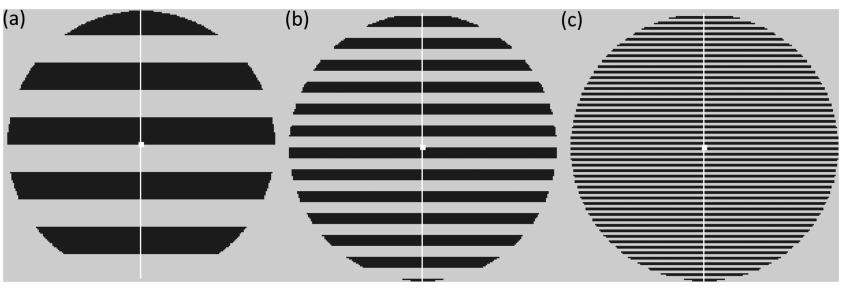

FIGURE 1 Pattern glare stimuli: left to right, thick (0.37 c/deg), medium (3 c/deg) and thin (12 c/deg) gratings with a central fixation and vertical dividing line. Note that the images shown here are representative of the stimuli but have been rendered to aid visibility in print

ethical concerns, participants had the option to turn off stimuli for the remaining duration of a trial by pressing a key; only three did and then only once each. Trials with stimulus hides were not automatically marked for removal. Reasoning that only a small number of epochs were affected and that these would most likely contain only small random variations close to baseline, we retained these epochs, but see supporting information for more justification. At the end of each block, participants were shown the three stimuli in turn and asked to rate the extent to which they had experienced a range of possible pattern glare symptoms (Wilkins et al., 1984); however, these were not analysed. After each block and at the end of the experiment, participants had a further resting period of 5 min, during which they were requested to close their eyes and relax. They were also asked if they were willing to continue at each break. Stimulus order and the number of onsets per trial were counterbalanced between participants.

2.4 | Analysis

2.4.1 | Discomfort ratings and questionnaires

Working with the 39 participants who completed the study, we computed mean discomfort ratings for each participant and stimulus type across the three blocks. Discomfort ratings tend to co-vary across the stimulus types, so we computed a discomfort index for each participant by subtracting mean discomfort ratings for the thick and thin stimuli from those for the medium stimulus. High scores on this index identify those participants who find the medium stimulus relatively uncomfortable compared with the two control stimuli. Overall scores for the CHi and VDS were computed according to the instructions for those tools. Finally, data for headache frequency, intensity and duration and the experience of sensory aura were extracted from the HGHQ. These seven measures have very different ranges, so we standardised each variable before entering them into a factor analysis, which identified three factors based on a Scree plot analysis. Following a Varimax rotation, the three factors were identified as visual stress (predominantly a combination of the CHi, VDS and aura), headache (frequency, intensity and duration) and discomfort (discomfort index). This factor structure is not surprising given the nature of the variables included, but the analysis also served to provide uncorrelated factors to aid the subsequent mass univariate analysis (MUA). Factor scores were computed using the regression method from coefficients shown in Section S1 of the supporting information, where we also describe the factor analysis in more detail. We included all 39 participants in the factor analysis because it benefits from larger datasets.

2.4.2 | ERP pre-processing

We decimated the EEG data from a sampling rate of 2048 to 512 Hz using the BioSemi toolbox. EEGs were then band-pass filtered using a second-order Butterworth filter with a pass band of 0.1 to 30 Hz (½ power −3 dB, fall-off at 12 dB per octave; for prior precedent for this choice, see Luck, 2014; Tanner et al., 2015). Data for each onset were epoched between −200 and 1200 ms relative to stimulus onset, referenced to the average of all electrodes and baseline corrected based on the 200-ms period prior to stimulus onset. Eye-blink artefacts were removed using independent component analysis (ICA), with ICA components associated with eye blinks removed and the dataset reconstructed. The crown electrodes (A11, A12, A13, A14, A24, A25, A26, A27, B8 and B9) were removed to further reduce the presence of muscle and eye-movement artefacts (Chennu et al., 2013), in line with previous work (Shirazibeheshti et al., 2018) who argue that this additional noise may confound MUA. The data were then re-referenced to the new electrode set. Data for individual onsets were deleted if any channel exceeded a ±100-μV threshold, thus removing large artefacts such as movement. The data for each participant were split into 27 bins, one for each stimulus type (thick, medium or thin) and Onset number (1 to 9). Finally, we discarded data from Onset 9—the number of onsets varied between 7 and 9 on each trial, so the occurrence of the ninth onset was rare, making these data unreliable. Tallying across onset number, three participants who did not have at least 20% of usable stimulus repeats per stimulus type were removed (decided a priori). However, in practice, those participants who were included had greater numbers of useable repeats (epochs). The mean (SD) total epoch count for Onsets 1 to 8 was 328.12 (41.85). For Onset 1 alone the mean epoch count was 39.18 (7.48). For Onsets 2–8 the mean total epoch count was 288.94 (37.41). In addition, one participant was removed because they had an artefact that could not be removed, and a further participant was removed because they had EEGs that were flat (i.e. equipment malfunction). We drew a logical distinction between the first stimulus onset in each trial (where the observer was unaware of the stimuli to be presented) and the remaining onsets (where the participant was able to anticipate the stimulus) and thus analyse Onset 1 separately from Onsets 2–8, the latter being combined so as to aggregate over the maximum number of onsets.

2.4.3 | Mass univariate analysis

A MUA was conducted in SPM-12 (Wellcome Trust Centre for Neuroimaging, London, England) on three-dimensional images (two of space, one of time) derived from the ERP data. Images were created using the data for each stimulus type (thick, medium, and thin). A contrast image was created based on what we call the pattern glare index (PGI). This index enables us to focus our analysis on regions of the data volume where the clinically relevant, medium stimulus exhibits an extreme response relative to the thick and thin stimuli.

$$\mathrm{PGI} = \text{medium image} - (\text{thick image} + \text{thin image})/2.$$

Then, we used the factor scores derived from the factor analysis as parametric regressors in the MUA, excluding factor scores from the five participants whose ERP data failed our screening tests.

This analysis focussed on the evoked response generated by a stimulus onset, which will be strongest at posterior regions of the scalp. To do this, we limited our analysis in two ways. First, we calculated an overall window of analysis in time considering only that portion of the grand average ERP waveform that deviated from baseline. This window was used to seed the subsequent region of interest (ROI) analysis. Second, we calculated two 3D ROIs in order to capture the P1 and subsequent ERP features that are central to our hypotheses.

The initial window of analysis was calculated as follows. ERPs are typically characterised by a series of positive and negative excursions from baseline, which correspond to the stimulus evoked onset transients, before the time-series settles back, and we wanted to capture only this period. To do this, we focussed on the aggregated average (Bowman et al., 2020; Brooks et al., 2017) across the three stimulus conditions (for Onsets 2–8). ROIs can be identified on the aggregated average, without inflating false-positive rates, since it does not reflect condition (i.e. stimulus) differences, which for us amounts to the PGI (Bowman et al., 2020; Brooks et al., 2017).[1] However, an initial inspection of our data revealed that the aggregated average did not settle back to baseline but rather fell to a constant, positive DC level. Thus, working with the aggregated average at electrode A23 (Oz), we captured the period from the first statistically significant deviation from baseline (zero) until the aggregated average finally fell to below statistical significance compared with the DC level. We first calculated the DC level from a period of 400-ms duration taken well after the end of the evoked transients. We took the mean value of all participants over this period. The window of analysis was then found by calculating confidence intervals across participants at each time point weighted by the number of valid trials.[2] We used the following equations for the weighted CI at each time point:

$$\mu_\omega = \frac{\sum_{i=1}^{n} x_i . m_i}{\sum_{i=1}^{n} m_i}$$

$$\overline{m} = \frac{\sum_{i=1}^{n} m_i}{n}$$

$$\sigma_\omega = \sqrt{\frac{\sum_{i=1}^{n} \frac{x_i^2 . m_i}{\overline{m}} - n\mu_\omega^2}{n-1}}$$

$$C_{95} = \mu_\omega - \frac{t_{95,n-1}\,\sigma_\omega}{\sqrt{n}}$$

where μ_ω is the weighted mean, σ_ω is the weighted standard deviation, C_{95} is the confidence interval, n is the number of participants, $t_{95,n-1} = 1.7$ is the critical t value for a one-tailed 95% confidence interval, x_i is the value of the ERP for the ith participant, m_i is the number of valid trials for that participant and $\overline{m}$ is the mean number of trials per participant. The lower CIs were compared with zero at the start of the ERP trace working forward and to the DC level at the end of the trace working backwards, yielding a window of analysis between 56- and 256- ms. This time window was used in the MUA analysis of the factor intercept and to seed our second ROI.

We next constructed ROIs using two methods. Our first ROI targeted the P1 excursion and was based a priori on the literature concerning this ERP feature (Bruyns-Haylett et al., 2017; Di Russo et al., 2002; Vogel & Luck, 2000; Zhang et al., 2013) resulting in an ROI volume centred on co-ordinates $x = 0$ mm, $y = -84$ mm, $t = 101$ ms with dimensions length = 92 mm, width = 42 mm and time = 62 ms (for explanation, see supporting information). Note also that Adjamian et al. (2004) located MEG sources in response to similar stimuli in the occipital pole.

[1]Indeed, it is straightforward to show that the aggregated average and the PGI are orthogonal: The dot product of the corresponding contrast vectors, [1/3,1/3,1/3] for the aggregated average and [1,-1/2,-1/2] for the PCI, is equal to zero.

[2]This weighting generates the Aggregated Grand Average of Trials (Brooks et al., 2017), upon which regions of interest can be selected without inflating type-I error rates in the presence of trial-count asymmetry.

Our second ROI targeted the ERP components subsequent to P1. The best locations and time period to capture such features are less well determined in the literature, so we took a different approach using an orthogonal contrast to determine an ROI (Bowman et al., 2020; Brooks et al., 2017). We used our analysis of the mean/intercept in the MUA (see Section 3) to produce an ROI mask for further analysis; Section S3 of the supporting information gives further justification for the validity of this approach. To this end, we applied a *t*-threshold of 5.55 (which corresponded to $p < 0.001$) to the intercept image to capture a coherent space–time mask for our second ROI. In practice, this ROI captures posterior electrodes in the period of the N1 excursion.

We used one-sample *t*-tests to demonstrate that individual regression coefficients (for our factors and intercept) are statistically different from zero. Analyses of the mean/intercepts were run two-tailed, but, then, analyses over factors were run one-tailed. This is because the direction of the effect that defined the ROI (based on prior precedent for P1 and mean/intercept for N1) governed the direction of interest for each factor effect. For example, if medium were largest for the mean/intercept, a positive correlation with a factor is the only theoretically plausible finding. This is because higher on the factor corresponds to a greater deficit, and our central hypothesis is that medium will induce a more extreme response from more impaired participants.

We did not perform statistical inference on our time-frequency plots. This is because any such analysis would be confounded by double dipping (Kriegeskorte et al., 2009), since we are interested in time-frequency features (including ROIs) that correspond to statistically significant effects observed in our time-domain (ERP) analyses. Accordingly, we view our time-frequency analyses as exploratory, but the statistical robustness of our findings rests upon our ERP analyses.

2.4.4 | Data visualisation

MUA treats each factor as a continuous variable and looks for statistically significant relationships between space–time maps and each factor. This approach produces space–time maps for the factors of concern but is of limited use for visualising the underlying ERPs. It also emphasises those participants who score at the extremes on each factor. We therefore placed our participants into two groups for each factor based on median splits of the factor scores. We then derived weighted ERPs for each (median split) group based on the absolute deviation of the factor scores from the median (a positive scalar) for each participant multiplied by the amplitude at each time point in the ERP matrix. To avoid shifting overall levels, we first subtract the median value at each time point, then calculate the weighted average before adding the median value back in. In this way, we scaled the ERPs according to the corresponding factor loadings in order to provide a visualisation that was more representative of the parametric regressor inferences of the MUA (see supporting information for unweighted ERPs). These groupings differed between the factors.

2.4.5 | Time-frequency analysis

We followed up our main MUA analysis with a time-frequency analysis to better understand the origin of one of our effects. To avoid edge effects during wavelet fitting, we expanded our EEG analysis window to include the −500- to 0-ms period. For each participant, we then examined amplitude and intertrial phase coherence for frequencies in the range 5–40 Hz using five-cycle Morlet wavelets at 1-Hz intervals. The results were then cropped between −100 and 800 ms, baseline rescaled using a logR ratio function to the (−100 to 0 ms) baseline window and then averaged. We present the results between 5 and 11 Hz. A further analysis of the lower frequencies used a three-cycle wavelet to improve temporal resolution.

3 | RESULTS

In summary, MUA finds statistically significant peaks and/or clusters of activity across the scalp and through time. This represents a large number of data points so MUA corrects for multiple comparisons to avoid inflation of the family-wise error rate (FWE correction). Peak effects refer to strong but isolated spikes of activity, whereas cluster effects may be weaker but extend over larger portions of space or time. We used MUA to test deflections in the PGI considering both mean/intercept effects, which do not depend on factor scores and factor-based contrasts which do. To limit the total number of comparisons made, this analysis was done in ROIs derived either from the literature (P1 effect) or from a window of statistically significant activity in an orthogonal contrast (N1 effect). For visualisation, we then extracted ERPs for the three stimuli separately at representative electrode locations. These were weighted by factor scores where relevant and are shown unweighted in the supporting information.

Considering mean/intercept effects, we found a peak effect in Onsets 2–8 (two-tailed $p < 0.001$, Figure 3) whereby the typical posterior N1 deflection at around 180 ms was replaced by an extended positive plateau for

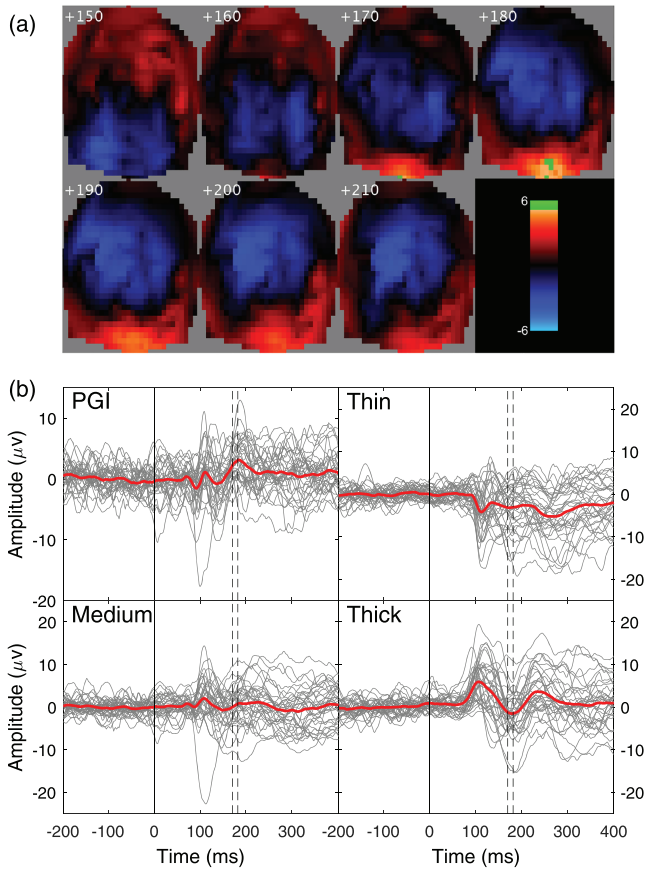

FIGURE 2 Topographic maps and event-related potentials (ERPs) for mean/intercept on Onset 1. (a) Topographic maps showing *t*-values based on the mean/intercept of the pattern glare index (PGI). Map values (indicated by colour scale) are shown in green when *t*-values exceed the threshold for statistical significance based on one-sample, one-tailed tests, FWE corrected at the peak level, for the period 150–210 ms in 10-ms intervals. (b) ERPs representing Onset 1 for medium, thick and thin stimuli and the PGI at electrode Oz. Faint lines show individual ERPs; thick red lines show group means. Vertical dashed lines show start and end of statistically significant effects. Positive is plotted up

medium-frequency stimuli. A similar, but smaller effect was seen for Onset 1 (two-tailed $p = 0.054$, Figure 2) which we consider worthy of report given the lower trial counts.

Considering the factor contrasts, we found no effects for the visual stress factor. The discomfort factor was associated with twin peak effects, located at lateral-occipital electrodes at around 100 ms (one-tailed $p = 0.027$ and 0.036, Figure 4); visualised as an emphasised P1 ERP component for those high on the discomfort factor in response to the medium stimulus. The headache factor was associated with a localised cluster effect located near the occipital pole at around 180 ms (one-tailed $p = 0.047$, Figure 5). This was visualised as a positive deflection in place of the N1 for the high group in response to the medium stimulus, whereas those low on the factor showed a more typical N1 deflection.

3.1 | Intercept effects

Figure 2a shows the results of the MUA for the mean/intercept for Onset 1 data only showing a FWE-corrected peak level effect ($z = 4.46$, $d = 0.92$ [at maximum voxel], $t(30) = 5.37$, $p = 0.027$, one-tailed; $p = 0.054$ two-tailed), at around 180 ms and centred at Oz. Figure 2b shows individual ERPs for all stimuli and the PGI index along with group means (in this case unweighted) at this electrode. Recalling that the MUA analysis was conducted on the PGI (not raw ERPs), the excursion occurred in the N1 period, where thick and thin exhibit a minimum whereas medium undergoes what appears to be an early P2 deflection. Individual traces are noisy as might be expected given the relatively low trial counts in the Onset 1 data; however, clear differences between stimuli can be seen and the trough in most of the traces for the thick stimuli at around 180 ms is clearly absent for the medium stimulus for most participants.

MUA intercept results for Onsets 2–8 showed a peak at 179 ms at Oz ($z = 6.19$, $d = 1.53$ [at maximum voxel], $t\ (30) = 8.94$, $p < 0.001$, FWE corrected at the peak level; Figure 3). Individual traces show clear P1-N1-P2 components in response to thick stimuli, which are synchronised across participants. The position of the N1 and P2 components in response to the medium stimuli is much less reliable leading to an apparent absence of an N1 component in the group mean. Interestingly, the ERP for Onsets 2–8 (Panel b) appears elevated relative to that for Onset 1 (Figure 2b), perhaps due to smaller N1 components. The late DC shift referred to above is also visible from around 350–400 ms in the ERPs for thick and medium stimuli but is most prevalent in a subset of participants.

3.2 | Factor effects

Figure 4 shows the MUA results for Onset 1 on the discomfort factor based on the a priori P1-ROI revealing two peaks at 97 ms (Panel a) centred on electrodes A20 (Panel b; $z = 3.77$, $d = 0.74$ [at maximum voxel], $t(30) = 4.31$, $p = 0.027$, one-tailed) and A8 (Panel c; $z = 3.67$, $d = 0.72$ [at maximum voxel], $t(30) = 4.17$, $p = 0.036$, one-tailed; both FWE peak corrected, with small volume correction). Comparing participants above and below the median value on the discomfort factor (thick red and blue traces in Figure 4 respectively), both electrodes show

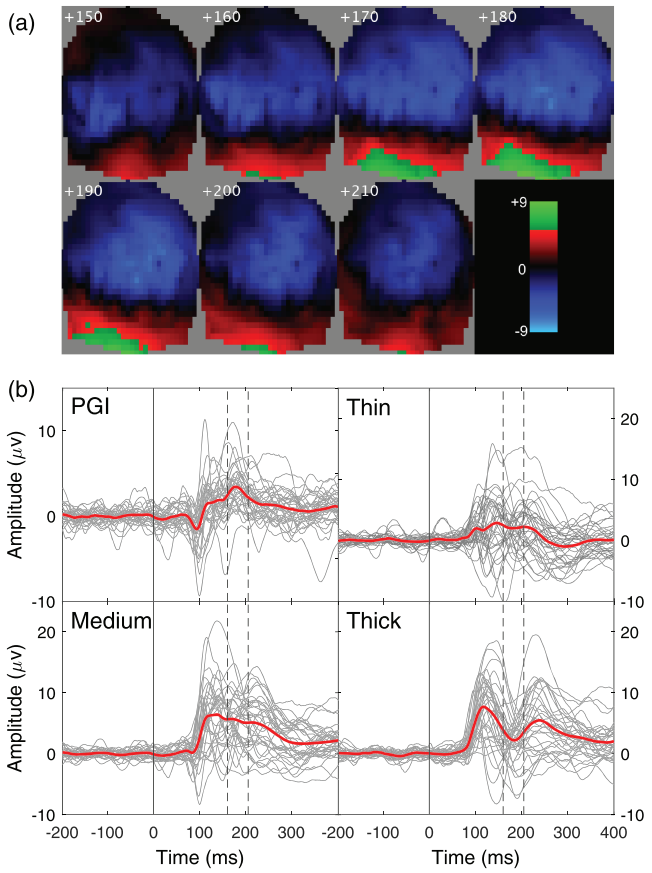

FIGURE 3 Topographic maps and event-related potentials (ERPs) for the mean/intercept on Onsets 2–8. (a) Topographic maps showing *t*-values based on the mean/intercept of the pattern glare index (PGI). Map values (indicated by colour scale) are shown in green when *t*-values exceed the threshold for statistical significance based on one-sample, one-tailed tests, FWE corrected at the peak level, for the period 150–210 ms in 10-ms intervals. (b) ERPs representing Onsets 2–8 for medium, thick and thin stimuli and the PGI at electrode Oz. Faint lines show individual ERPs; thick red lines show group means. Vertical dashed lines show start and end of statistically significant effects. Positive is plotted up

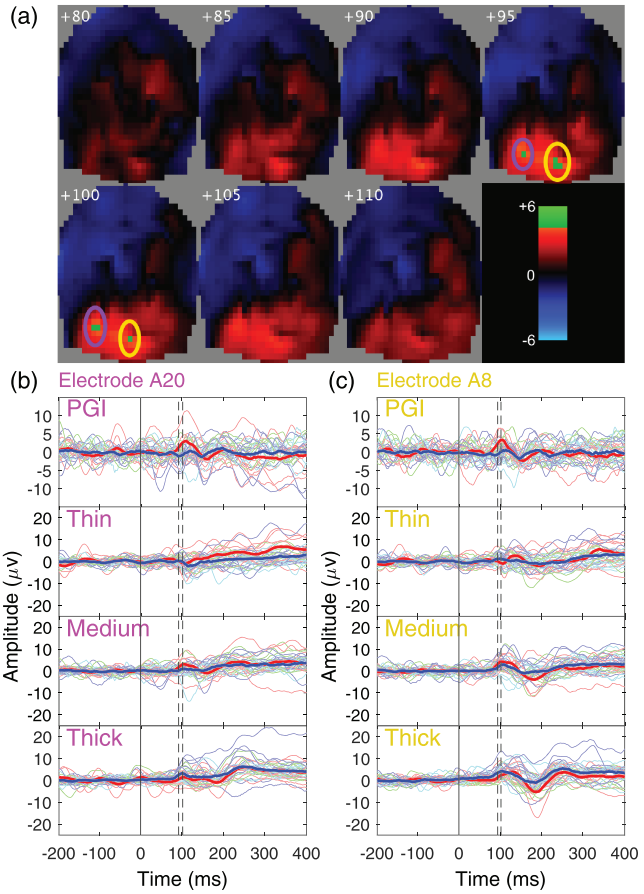

FIGURE 4 Topographic maps and event-related potentials (ERPs) for discomfort factor scores for Onset 1. (a) Topographic maps showing *t*-values based on the pattern glare index (PGI). Map values (indicated by colour scale) are shown in green when *t*-values exceed the threshold for statistical significance based on one-sample, one-tailed tests, FWE corrected at the peak level within an ROI derived a priori from the literature (see main text), for the period 80–110 ms in 5-ms intervals. Coloured ovals added to link clusters to ERPs. (b, c) ERPs on the discomfort factor for thin, medium and thick stimuli and the PGI for the statistically significant electrodes: A20 (magenta; panel b) and A8 (yellow; panel c) at the corresponding points in each cluster in (a). Faint lines show ERPs for individual participants with quartiles on the discomfort factor represented by red, green, cyan and blue traces (upper to lower quartiles, respectively). Thick lines show weighted means (see main text) based on a median split of the discomfort factor: red represents those high on the factor, blue—low. Vertical dashed lines show start and end of statistically significant effects. Positive plotted up

an elevated P1 component for medium-frequency stimuli that is present, on average, in the high-discomfort group but not those low on the factor. While there are some exceptions, this is borne, out in the individual participant data. High discomfort is associated with a strong P1 peak for the first appearance (Onset 1) of medium stimuli.

Figure 5 shows the MUA results for Onsets 2–8 on the headache factor based on the orthogonal contrast N1-ROI. We found a localised cluster ($z = 3.06$, $d = 0.57$ [at maximum voxel], $t(30) = 3.34$, $p = 0.047$, one-tailed, FWE cluster level corrected, with small volume correction) centred at electrode A29 comprising four voxels but lasting over 22 ms from 155 to 177 ms with a peak at 173 ms. Averaged ERPs (Panel b) suggest that either the N1 deflection is missing for the medium stimulus in the high-headache group or that the P2 is accelerated and perhaps somewhat variable in latency in the high group. We note that the timing of the P2 component

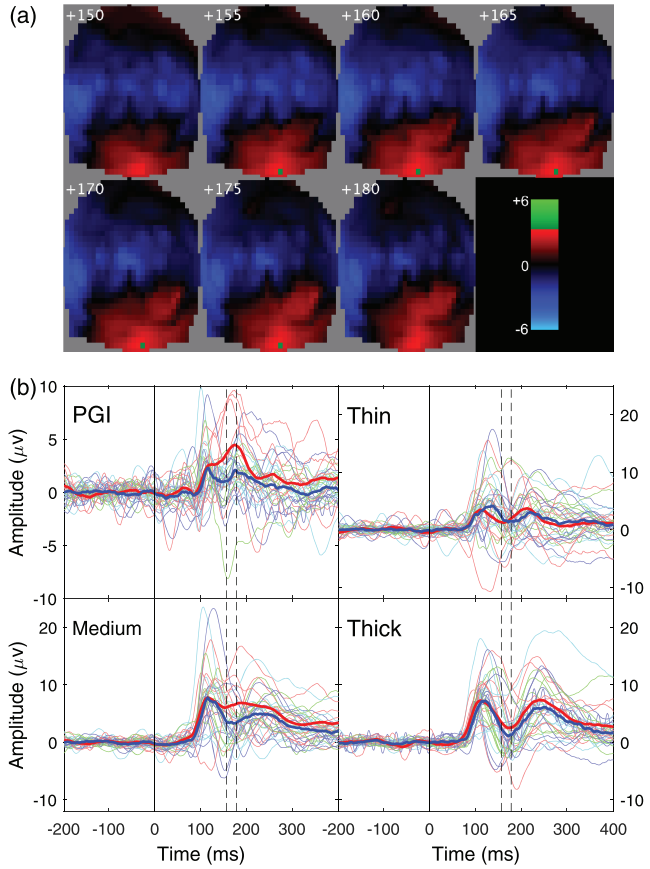

FIGURE 5 Topographic maps and event-related potentials (ERPs) for headache factor scores for Onsets 2–8. (a) Topographic maps showing *t*-values based on the pattern glare index (PGI). Map values (indicated by colour scale) are shown in green when *t*-values exceed the threshold for statistical significance based on one-sample, one-tailed tests, FWE corrected at the cluster level with small volume correction within an ROI based on an orthogonally derived mask from the mean/intercept of Onsets 2–8 (see main text), for the period 150–180 ms in 5-ms intervals. (b) ERPs on the headache factor for thin, medium and thick stimuli and the PGI for the statistically significant electrode (A29). Faint lines show ERPs for individual participants with quartiles on the discomfort factor represented by red, green, cyan and blue traces (upper to lower quartiles, respectively). Thick lines show weighted means (see main text) based on a median split of the headache factor: red represents those high on the factor, blue—low. Vertical dashed lines show start and end of statistically significant effects. Positive plotted up

appears less reliable across participants for medium versus thick stimuli although it is hard to discern if this effect is worse for the high group. We explored these two possibilities further using a time-frequency analysis. Such an analysis allows the comparison of the strength (amplitude) and temporal (phase) coherence of individual Fourier components in the ERPs across trials. It can thus distinguish between low-amplitude signals and high-amplitude signals with poor temporal coherence, which are indistinguishable in an ERP. It is thus much more sensitive to temporal jitter. As time-frequency analysis calculates average power and intertrial phase coherence across trials and participants, an absence of N1 at the trial level would likely result in reduced theta band power for the high-group with medium stimuli. This is because theta is the dominant band for the P1-N1-P2 complex. In contrast, if the apparently weak N1 were due to variability in the timing of P2, we would expect power to be unaffected but intertrial phase coherence to be weak in this time period.

Figure 6 shows time-frequency power plots for the high-headache group for the three stimuli. We have marked the ROI in the relevant power plots in Figure 6. Power is about as high for the medium stimulus in the theta band (around 7 Hz) as for the thick stimulus. That is, the power plots for thick and medium stimuli are similar, despite the lack of visible N1 in the medium ERP. Figure 7 shows intertrial phase coherence plots for the high (Figure 7a–c) and low (Figure 7d–f) groups for each type of stimulus. Phase coherence in the theta band in the relevant window is similar for the thick and medium stimuli in the low-headache group but weaker for medium stimuli than thick in the high-headache group, suggesting that temporal jitter (Chennu et al., 2009) in the timing of the P2 is responsible for the altered ERPs. Another way of thinking about this would be that for those high on the headache factor; in the relevant time window, the medium condition is exhibiting an induced response (i.e. high power, but less locking to the stimulus), while the thick condition is exhibiting a more typical evoked response (i.e. high power, with strong stimulus locking). The fact that there is low phase consistency across trials at the relevant time-frequency point for thin stimuli does not confound our argument. That could simply be explained by the lower power for thin, which would cause a loss of intertrial coherence because the noise in the data has a greater impact on the measurement of phase, when the signal has low amplitude (Chennu et al., 2009).

To provide converging evidence for our jittered-P2 hypothesis for the high-headache group's response to the medium stimulus, we conducted a power analysis on the grand averages. That is, we computed power after averaging rather than before. We would now expect to find a fall in signal level theta power for medium relative to thick at the relevant time period despite the absence of such a dip in the normal power-plot of Figure 6. Using a smaller three-cycle wavelet (which improves temporal resolution but reduces frequency resolution), we indeed observe a loss in theta power at around 185 ms as expected (see Figure 8).

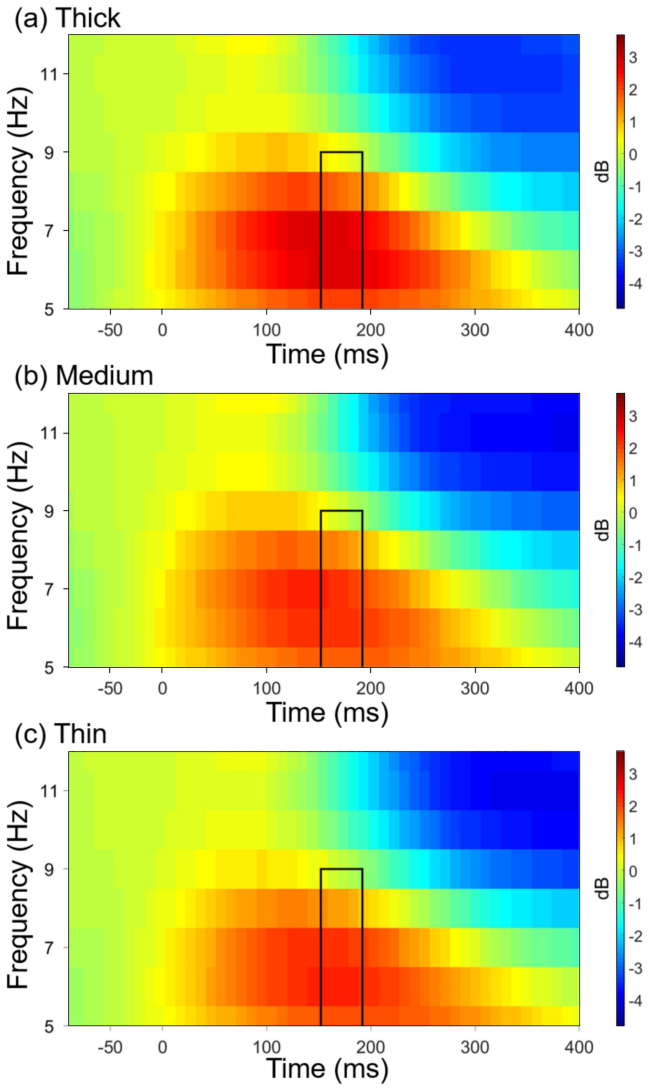

FIGURE 6 Time-frequency analysis for those high on the headache factor. Power as a function of oscillation frequency and time is shown: (a) thick stimulus, (b) medium stimulus and (c) thin stimulus at electrode A29. Colours represent power in dB, which was calculated using a five-cycle wavelet. Box shows window of interest based on significance window for headache factor from the time-domain

4 | DISCUSSION

We considered the neural correlates of visual stress and headache using ERPs finding that state measures of visual stress (the PGI) correlate with stronger P1 component for the first presentation of a repeated stimulus only, whereas headache proneness correlates with erratic timing of the P2 component leading to an apparent absence of the N1 component. Visual stress has been associated with a range of conditions including migraine, and this condition, in particular, is a major cause of disability and lost potential in the working age population. Therefore, a better understanding of the neural factors that are associated with headaches may help to reduce their impact. Migraineurs are known to be sensitive to striped stimuli of a particular midrange spatial frequency. In the present study, we considered evoked responses to such stimuli in the general population and related them to three factors: visual stress, a tendency for headaches and discomfort in response to aggravating stimuli. These factors were, by construction, uncorrelated. We found effects for the headache and discomfort factors operating at different times in terms of stimulus presentation and on different components in the ERP. Both these effects are new and would benefit from replication: While both are statistically significant ($p = 0.027$ and $p = 0.047$), even samples of size 34 (which is a good size for neuroimaging) are subject to substantial error (Lorca-Puls et al., 2018).

The state measure discomfort showed an effect only for the first presentation of the stimulus (Onset 1), suggesting that this factor may relate to the initial response to a new stimulus and habituate thereafter. The second factor combined headache frequency, intensity and duration and was associated with effects only for subsequent presentations of the stimulus (Onsets 2–8). The separation between these effects across factor, time (from stimulus onset) and electrode sites suggests that they represent distinct physiological phenomena in the way the first stimulus presentation and the remaining onsets are processed. We will discuss these effects more fully below after discussing the stimulus-driven effects that were not factor dependent.

4.1 | Stimulus-driven mean/intercept effects

The mean/intercept effect for Onset 1 was weak. Thus, at present, this effect needs to be treated with caution. This said, we have included the effect, since it somewhat mirrors what we see for Onsets 2–8, which is a more highly powered condition (as it involves many more stimulus repetitions), affording it some face validity. When looking at the mean intercept of both Onset 1 and Onset 2–8 trials, the most salient feature is that the window of time and position of the effect is similar for both subdivisions of trials, which suggests an underlying connection. The P2 elicited by Onset 1 (see Figure 2) seems to be accelerated in the medium condition relative to the thick/thin conditions, and visually, there is attenuation of N1 in Onsets 2–8 for medium stripes relative to thick (see Figure 3), which could also relate to an accelerated P2. The similarity between this result for all participants and the N1-P2 effects found for the high-headache group on

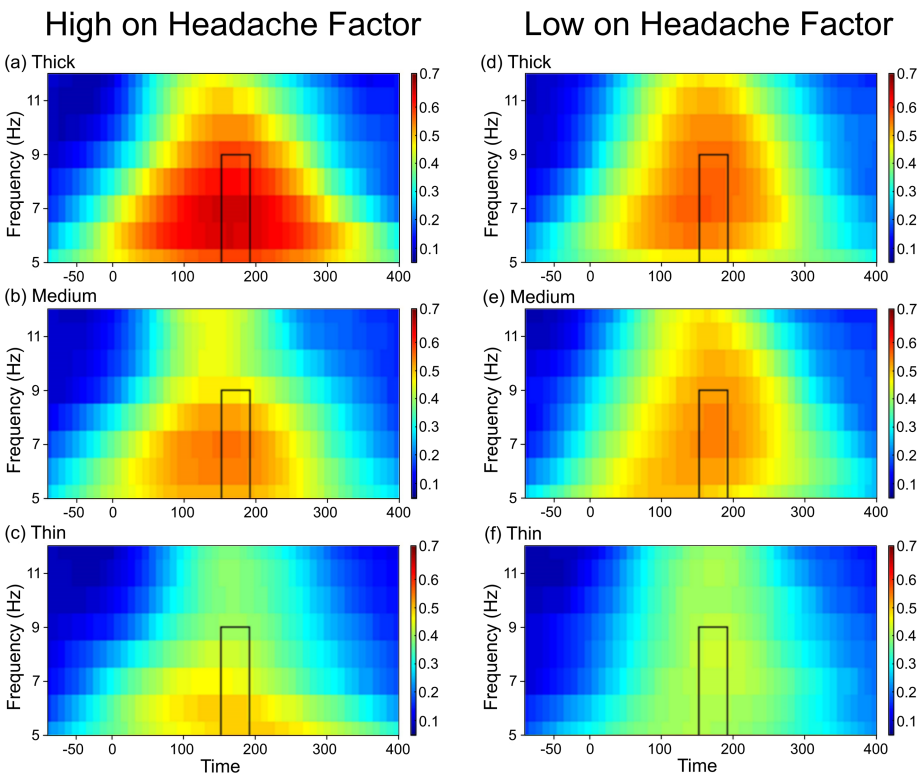

FIGURE 7 Time-frequency analysis for those high (left) and low (right) on the headache factor, showing intertrial coherence as a function of oscillation frequency over time for Onsets 2–8: (a, d) thick stimulus, (b, e) medium stimulus and (c, f) thin stimulus at electrode A29. Colours represent intertrial coherence, calculated using a five-cycle wavelet. Box shows window of interest based on significance window for headache factor from the time-domain

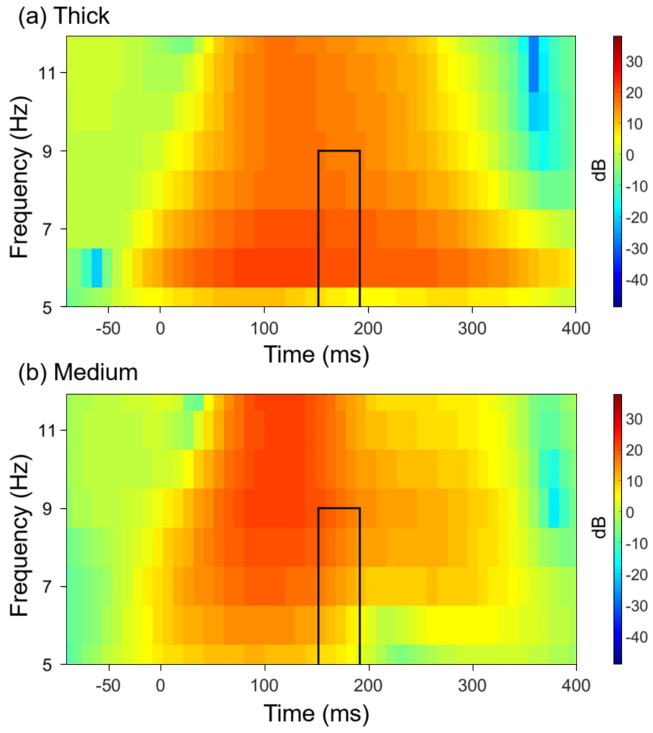

FIGURE 8 Time-frequency plots for those high on the headache factor calculated on grand averages, (a) thick stimulus and (b) medium stimulus at electrode A29, analysed with three-cycle wavelets. Box shows window of interest based on significance window for headache factor from the time-domain. Colours represent power in dB

Onsets 2–8 only (see Figure 5 and later) is striking. This may suggest that the effect is driven by the medium stimulus regardless of participant characteristics but is accentuated in the high-headache group. The visual N1 is considered important in modulating spatial attention (Hillyard et al., 1998; Mangun, 1995) and discriminative processing (Hopf et al., 2002; Vogel & Luck, 2000). However, one explanation to account for a reduction of the N1 attentional effect in sequences of bilateral stimuli (Heinze et al., 1990) is that physiological refractoriness due to the stimulus repetition might reduce the N1 amplitude (Luck et al., 1990). Additionally, N1 is affected by stimulus properties such as brightness of stimulus and intensity (Carrillo-De-La-Peña et al., 1999; Munte et al., 1995), although N1 amplitude is generally higher for stronger stimuli. We will return to this point when discussing the visually weak N1 component found for our high-headache group.

4.2 | Discomfort

The discomfort factor reflects a state measure of how comfortable (low scores) or uncomfortable (high scores) participants found the medium stripes relative to the other stimuli during the course of the experiment. We found a stronger P1 for the high-discomfort group compared with low discomfort in response to the medium striped stimuli (see Figure 4). Specifically, for the high-

discomfort group, the medium stimuli elicited stronger P1 than the other stimuli. This was not so for the low-discomfort group. This supports our hypothesis that medium stripes would elicit different early ERP components compared with thick and thin but only in individuals showing evidence of visual sensitivity. Strong occipital P1 has been associated with higher luminance, suggesting that stronger stimuli may elicit a stronger P1 at posterior electrodes (Carrillo-De-La-Peña et al., 1999; Munte et al., 1995). In the context of our study, those with cortical hyperexcitability may respond more strongly to certain stimuli (particularly those that are aggravating) as if they were presented at higher strength. This group might also be more likely to find those stimuli uncomfortable. Thus, hyperexcitability alone could produce the enhanced P1 in the high-discomfort group. In addition, P1 is associated with spatial attention (Luck et al., 1990; Luck & Hillyard, 1994). In particular, P1 is reduced for unattended stimuli (Mangun & Hillyard, 1991; Munte et al., 1995; Van Voorhis & Hillyard, 1977). Therefore, in our experiment, the lack of P1 in the low-discomfort group may also be because these participants were able to quickly shift attention away from this aggravating stimulus, thus avoiding discomfort. In contrast, the high-discomfort group may have been unable to withdraw attention from the medium stimulus.

Our P1 differences are specific to Onset 1, that is, the initial presentation of each stimulus type in a series of repeated presentations. Of the two onset groups, Onset 1 has the least statistical power so the lack of any P1 effect for Onsets 2–8 combined (and indeed for each of these onsets when considered individually; see supporting information) suggests a genuine habituation effect, not a lack of power. However, we think it unlikely that discomfort itself habituates between onsets as these ratings increased over the course of the experiment, statistically significantly so for the medium stimulus (Greenhouse–Geisser, $F = 4.395$, $d.f = [1.497, 55.5374]$, $p = 0.016$, $\eta_p{}^2 = 0.106$). Noting that the P1 has been associated with surprise (Lassalle & Itier, 2013; Utama et al., 2009); it seems more likely that even the high-discomfort group are able to ignore or attenuate the impact of the medium stimulus when they are expecting it to occur—in this group at least, habituation of P1 is effective.

4.3 | Headache

The headache factor is a trait measure recording the participant's proneness to long, intense and frequent headaches. The high-headache group shows an atypical N1 for the medium stimuli in Onsets 2–8 combined. The effect was not seen in Onset 1, and an analysis of individual onsets showed it was present in Onsets 3 to 8 but not Onsets 1 or 2 (see supporting information). This may be due to an absent or attenuated N1 or an accelerated and temporally unreliable P2. Our time-frequency analyses suggest that the P2 account is more likely, but we cannot dismiss the N1 account entirely. Here, we briefly outline the implications of an attenuated N1 before discussing P2 more fully.

The low-headache group showed a strong N1 component for medium stimuli, but the high-headache group showed a slight opposite polarity deflection in the same period in weighted ERPs (see Figure 5b) and a reduced amplitude N1 in the unweighted ERPs (supporting information). At first sight, this result appears opposite to that of Fong et al. (2020) who found migraine sufferers to have more negative ERPs around 200 ms (equivalent to our N1). However, they did not use repeated onsets and so could not have revealed our positive going effect for Onsets 2–8. We did find a non-significant negative going effect for medium stimuli at electrode Oz at around 200 ms for Onset 1, and this may represent Fong et al's effect, which would be magnified in their study by higher trial counts for the first (only) stimulus repetition and a more clearly defined patient group (see supporting information).

Occipital N1 is also linked to stimulus intensity (Munte et al., 1995), with higher amplitude and shorter latencies associated with stronger stimuli. The amplitude of the occipital N1 has also been linked to attention, with a stronger N1 at attended locations (Luck et al., 2000). Thus, assuming a link between cortical-hyperexcitability and headaches, neither a hyperexcitability account nor failure to withdraw attention would account for low N1 amplitudes in our high-headache group. However, in the auditory domain, reduced N1 amplitude has been associated with repetition suppression (Hsu et al., 2014). It is possible then that the high-headache group is successful in suppressing the repeated medium stimuli, whereas the low-headache group does not feel the need to suppress this stimulus as, for them, it may be weaker in the first place. This would imply that the high-headache group habituates to the medium stimulus. There is conflicting evidence in the literature showing both that those with migraine fail to habituate to repeated stimulation of the same stimulus (Brighina et al., 2009; Brighina et al., 2016; Schoenen et al., 1995) and conversely that habituation may be present in migraineurs (Omland et al., 2013, 2016). However, this habituation account seems unlikely in the light of the time-frequency analysis described above and discussed next.

Our time-frequency analysis suggests that EEG power is relatively stable between the medium and thick stimuli in all frequency bands and in particular in the theta band over the period of time for which ERPs for the two stimuli most differ in the high-headache group (see Figure 6). Reduced theta power, as might be associated with an absent N1, does not explain our data. However, intertrial phase coherence is reduced for the high-headache group viewing medium stimuli during the critical period around 165 ms after stimulus onset. This suggests that theta phase coherence (locking) may be weak in this group for this stimulus. Intertrial theta phase coherence has been associated with the P2 component (Freunberger et al., 2007), and it is possible that variability in the timing of the P2 component, from trial-to-trial or between participants, spreads this component in time, masking the N1 in the ERP. We now further explore the role of the P2 component.

The P2 component has been associated with a number of top-down attentional tasks such as visual search (Luck & Hillyard, 1994). This association with top-down processing makes modulations of P2 an unlikely candidate in our study where the attentional load is minimal. However, we note that variations in P2 latency have been found across a range of conditions where neural inhibition is potentially compromised, including ADHD (Johnstone et al., 2009), Schizophrenia (Shin et al., 2010) and ageing (Bourisly & Shuaib, 2018). Mostly, P2 onset is delayed in these conditions, which would not compromise the N1 region, but we note first that our high-headache group may not all have been migraineurs and second that migraine is not necessarily associated with poor inhibition but rather with an imbalance between excitation and inhibition. For example, Shepherd and Joly-Mascheroni (2017) reported stronger inhibitory illusions in those with migraine. It is possible therefore that our headache group exhibits unreliable P2 and poor intertrial theta phase coherence around the P2 time period, with an advanced, rather than delayed, P2 on some trials. In the auditory domain, the phase of low-frequency EEG components has been associated with stimulus identity (Ng et al., 2013) and we speculate that poor phase coherence in the theta band may be due to the variable appearance of the medium grating due to the distortions and illusory perceptions that this stimulus is known to induce. Importantly, theta phase connectivity has been associated with increased frequency of epileptic attacks (Douw et al., 2010). Given our participants' high scores on the headache factor, there may be overlap between some of these individuals and the migraine population. However, more work is required to pin-point the cause of the absent N1/unreliable P2 and relate it to inhibitory mechanisms.

5 | CONCLUSION

In conclusion, we found two factors related to altered ERPs. Those scoring high on the discomfort factor exhibited an increased P1 component for the medium stimulus relative to both the other stimuli and the low-discomfort group. This state measure may relate to cortical hyperexcitability making the stimuli appear more potent or to an inability to disengage attention. Those scoring high on the headache factor showed a difference in the N1-P2 time window consistent with an early/jittered P2 masking N1. This could relate to poor intertrial theta phase coherence and poorly regulated P2 timing but could also be evidence of successful suppression of repeated stimuli or habituation. The dissociation between these factors across time from stimulus onset, stimulus repeats and electrode sites suggests that they relate to distant neural processes. Given previous results suggesting that differences in hyperexcitability and habituation in migraine are underpinned by different physiological phenomena, future studies are needed to see whether our results are transferable to clinically diagnosed migraineurs.

ACKNOWLEDGEMENTS

We want to thank Guillaume Flandin for their help with SPM use and expertise. They also assisted in refining analysis code. We would also like to thank Sara Assecondi for assistance with EEG pre-processing and Cathy Ghalib for help with data collection. We were not funded for this research.

CONFLICT OF INTEREST

The authors report no competing interests.

AUTHOR CONTRIBUTIONS

AJT contributed to data collection, analysed the data, interpreted the results, wrote the first draft and contributed to later drafts. CEM contributed to experiment code, collected data, interpreted the results and contributed to all drafts. VL contributed to data analysis and reviewed final draft. HB conceived the study, interpreted the results and contributed to all drafts. AJS conceived the study, wrote experiment code, contributed to data analysis, interpreted the results and contributed to all drafts.

PEER REVIEW

The peer review history for this article is available at https://publons.com/publon/10.1111/ejn.15419.

DATA AVAILABILITY STATEMENT

The data that support the findings of this study are openly available in the UBIRA eData repository at

https://doi.org/10.25500/eData.bham.00000616, reference number 616.

ORCID

Austyn J. Tempesta https://orcid.org/0000-0001-5464-503X

Howard Bowman https://orcid.org/0000-0003-4736-1869

Andrew J. Schofield https://orcid.org/0000-0002-0589-4678

REFERENCES

Adjamian, P., Holliday, I. E., Barnes, G. R., Hillebrand, A., Hadjipapas, A., & Singh, K. D. (2004). Induced visual illusions and gamma oscillations in human primary visual cortex. *European Journal of Neuroscience*, *20*(2), 587–592. https://doi.org/10.1111/j.1460-9568.2004.03495.x

Afra, J., Cecchini, A. P., De Pasqua, V., Albert, A., & Schoenen, J. (1998). Visual evoked potentials during long periods of pattern-reversal stimulation in migraine. *Brain*, *121*(2), 233–241. https://doi.org/10.1093/brain/121.2.233

Aldrich, A., Hibbard, P., & Wilkins, A. (2019). Vision and hyper-responsiveness in migraine. *Vision*, *3*, 62. https://doi.org/10.3390/vision3040062

Ambrosini, A., & Schoenen, J. (2006). Electrophysiological response patterns of primary sensory cortices in migraine. *The Journal of Headache and Pain*, *7*(6), 377–388. https://doi.org/10.1007/s10194-006-0343-x

Badawy, R. A. B., Vorgin, S. J., Lai, A., & Cook, M. J. (2013). Patterns of cortical hyperexcitability in adolescent/adult—Onset generalized epilepsies. *Epilepsia*, *54*, 871–878. https://doi.org/10.1111/epi.12151

Beasley, I. G., & Davies, L. N. (2012). Susceptibility to pattern glare following stroke. *Journal of Neurology*, *259*(9), 1832–1839. https://doi.org/10.1007/s00415-012-6418-5

Bourisly, A. K., & Shuaib, A. (2018). Neurophysiologoical effects of ageing: A P200 ERP study. *Translational Neuroscience*, *9*, 61–66. https://doi.org/10.1515/tnsci-2018-0011

Bowman, H., Brooks, J. L., Hajilou, O., Zoumpoulaki, A., Litvak, V., Bowman, H., Brooks, J. L., Hajilou, O., Zoumpoulaki, A., & Litvak, V. (2020). Breaking the circularity in circular analyses: Simulations and formal treatment of the flattened average approach. *PLOS Computational Biology*, *16*(11), e1008286. https://doi.org/10.1371/journal.pcbi.1008286

Brainard, D. H. (1997). The Psychophysics Toolbox. *Spatial Vision*, *10*, 433–436.

Braithwaite, J. J., Marchant, R., Takahashi, C., Dewe, H., & Watson, D. (2015). The cortical hyperexcitability index (CHi): A new measure for quantifying correlates of visually driven cortical hyperexcitability. *Cognitive Neuropsychiatry*, *20*(4), 330–348. https://doi.org/10.1080/13546805.2015.1040152

Brighina, F., Cosentino, G., & Fierro, B. (2016). Habituation or lack of habituation: What is really lacking in migraine? *Clinical Neurophysiology*, *127*(1), 18–20.

Brighina, F., Palermo, A., & Fierro, B. (2009). Cortical inhibition and habituation to evoked potentials: Relevance for pathophysiology of migraine. *The Journal of Headache and Pain*, *10*(2), 77–84. https://doi.org/10.1007/s10194-008-0095-x

Brinciotti, M., Guidetti, V., Matricardi, M., & Cortesi, F. (1986). Responsiveness of the visual system in childhood migraine studied by means of VEPs. *Cephalalgia*, *6*(3), 183–185. https://doi.org/10.1046/j.1468-2982.1986.0603183.x

Brooks, J. L., Zoumpoulaki, A., & Bowman, H. (2017). Data-driven region-of-interest selection without inflating type I error rate. *Psychophysiology*, *54*(1), 100–113. https://doi.org/10.1111/psyp.12682

Bruyns-Haylett, M., Luo, J., Kennerley, A. J., Harris, S., Boorman, L., Milne, E., Vautrelle, N., Hayashi, Y., Whalley, B. J., Jones, M., & Berwick, J. (2017). The neurogenesis of P1 and N1: A concurrent EEG/LFP study. *NeuroImage*, *146*, 575–588. https://doi.org/10.1016/j.neuroimage.2016.09.034

Carrillo-De-La-Peña, M., Holguín, S. R., Corral, M., & Cadaveira, F. (1999). The effects of stimulus intensity and age on visual-evoked potentials (VEPs) in normal children. *Psychophysiology*, *36*(6), 693–698. https://doi.org/10.1111/1469-8986.3660693

Chennu, S., Craston, P., Wyble, B., & Bowman, H. (2009). Attention increases the temporal precision of conscious perception: Verifying the neural-ST2 model. *PLoS Computational Biology*, *5*(11), e1000576. https://doi.org/10.1371/journal.pcbi.1000576

Chennu, S., Noreika, V., Gueorguiev, D., Blenkmann, A., Kochen, S., Ibanez, A., Owen, A. M., Bekinschtein, T. A., & Bekinschtein, T. A. (2013). Expectations and attention in hierarchical auditory prediction. *Journal of Neuroscience*, *33*(27), 11194–11205. https://doi.org/10.1523/JNEUROSCI.0114-13.2013

Conlon, E. G., Lovegrove, W. J., Chekaluk, E., & Pattison, P. E. (1999). Measuring visual discomfort. *Visual Cognition*, *6*(6), 637–663. https://doi.org/10.1080/135062899394885

Connolly, J. F., Gawel, M., & Rose, F. C. (1982). Migraine patients exhibit abnormalities in the visual evoked potential. *Journal of Neurology, Neurosurgery & Psychiatry*, *45*(5), 464–467. https://doi.org/10.1136/jnnp.45.5.464

Coppola, G., Pierelli, F., & Schoenen, J. (2009). Habituation and migraine. *Neurobiology of Learning and Memory*, *92*(2), 249–259. https://doi.org/10.1016/j.nlm.2008.07.006

Coutts, L. V., Cooper, C. E., Elwell, C. E., & Wilkins, A. J. (2012). Time course of the haemodynamic response to visual stimulation in migraine, measured using near-infrared spectroscopy. *Cephalalgia*, *32*(8), 621–629.

Di Russo, F., Martínez, A., Sereno, M. I., Pitzalis, S., & Hillyard, S. A. (2002). Cortical sources of the early components of the visual evoked potential. *Human Brain Mapping*, *15*(2), 95–111. https://doi.org/10.1002/hbm.10010

Douw, L., van Dellen, E., de Groot, M., Heimans, J. J., Klein, M., Stam, C. J., & Reijneveld, J. C. (2010). Epilepsy is related to theta band brain connectivity and network topology in brain tumor patients. *BMC Neuroscience*, *11*(1), 103. https://doi.org/10.1186/1471-2202-11-103

Evans, B. J. W., & Stevenson, S. J. (2008). The pattern glare test: A review and determination of normative values. *Ophthalmic and Physiological Optics*, *28*(4), 295–309. https://doi.org/10.1111/j.1475-1313.2008.00578.x

Fong, C. Y., Law, W. H. C., Braithwaite, J., & Mazaheri, A. (2020). Differences in early and late pattern-onset visual-evoked potentials between self-reported migraineurs and controls. *NeuroImage: Clinical*, *25*, 102122. https://doi.org/10.1016/j.nicl.2019.102122

Freunberger, R., Klimesch, W., Doppelmayr, M., & Höller, Y. (2007). Visual P2 component is related to theta phase-locking. *Neuroscience Letters*, *426*(3), 181–186. https://doi.org/10.1016/j.neulet.2007.08.062

Friedman, D. I., & De Ver Dye, T. (2009). Migraine and the environment. *Headache: The Journal of Head and Face Pain*, *49*(6), 941–952. https://doi.org/10.1111/j.1526-4610.2009.01443.x

Friston, K. J., & Penny, W. (2003). Posterior probability maps and SPMs. *NeuroImage*, *19*(3), 1240–1249. https://doi.org/10.1016/S1053-8119(03)00144-7

Friston, K. J., Penny, W., Phillips, C., Kiebel, S., Hinton, G., & Ashburner, J. (2002). Classical and Bayesian inference in neuroimaging: Theory. *NeuroImage*, *16*(2), 465–483. https://doi.org/10.1006/nimg.2002.1090

Haigh, S. M., Chamanzar, A., Grover, P., & Behrmann, M. (2019). Cortical Hyper-Excitability in Migraine in Response to Chromatic Patterns. *Headache: The Journal of Head and Face Pain*, *59*(10), 1773–1787. https://doi.org/10.1111/head.13620

Haigh, S. M., Cooper, N. R., & Wilkins, A. J. (2015). Cortical excitability and the shape of the haemodynamic response. *NeuroImage*, *111*, 379–384. https://doi.org/10.1016/j.neuroimage.2015.02.034

Harle, D. E., Shepherd, A. J., & Evans, B. J. (2006). Visual stimuli are common triggers of migraine and are associated with pattern glare. *Headache: The Journal of Head and Face Pain*, *46*(9), 1431–1440. https://doi.org/10.1111/j.1526-4610.2006.00585.x

Heinze, H. J., Luck, S. J., Mangun, G. R., & Hillyard, S. A. (1990). Visual event-related potentials index focused attention within bilateral stimulus arrays. I. Evidence for early selection. *Electroencephalography and Clinical Neurophysiology*, *75*(6), 511–527. https://doi.org/10.1016/0013-4694(90)90138-A

Hillyard, S. A., Vogel, E. K., & Luck, S. J. (1998). Sensory gain control (amplification) as a mechanism of selective attention: Electrophysiological and neuroimaging evidence. *Philosophical Transactions Royal Society of London B*, *353*, 1257–1270.

Hopf, J. M., Vogel, E., Woodman, G., Heinze, H. J., & Luck, S. J. (2002). Localizing visual discrimination processes in time and space. *Journal of Neurophysiology*, *88*(4), 2088–2095. https://doi.org/10.1152/jn.2002.88.4.2088

Hougaard, A., Amin, F. M., Hoffmann, M. B., Rostrup, E., Larsson, H. B., Asghar, M. S., Larsen, V. A., Olesen, J., & Ashina, M. (2014). Interhemispheric differences of fMRI responses to visual stimuli in patients with side-fixed migraine aura. *Human Brain Mapping*, *35*(6), 2714–2723. https://doi.org/10.1002/hbm.22361

Hsu, Y.-F., Hämäläinen, J. A., & Waszak, F. (2014). Repetition suppression comprises both attention-independent and attention-dependent processes. *NeuroImage*, *98*, 168–175. https://doi.org/10.1016/j.neuroimage.2014.04.084

Huang, J., Cooper, T. G., Satana, B., Kaufman, D. I., & Cao, Y. (2003). Visual distortion provoked by a stimulus in migraine associated with hyperneuronal activity. *Headache: The Journal of Head and Face Pain*, *43*(6), 664–671. https://doi.org/10.1046/j.1526-4610.2003.03110.x

Huang, J., Zong, X., Wilkins, A., Jenkins, B., Bozoki, A., & Cao, Y. (2011). fMRI evidence that precision ophthalmic tints reduce cortical hyperactivation in migraine. *Cephalalgia*, *31*(8), 925–936. https://doi.org/10.1177/0333102411409076

IHS, Headache Classification Committee of the International Headache Society. (2018). The international classification of headache disorders, 3rd edition. *Cephalalgia*, *38*, 1–211.

Johnstone, S. J., Barry, R. J., Markovska, V., Dimoska, A., & Clarke, A. R. (2009). Response inhibition and interference control in children with AD/HD: A visual ERP investigation. *International Journal of Psychophysiology*, *72*, 145–153.

Kientz, M. A., & Dunn, W. (1997). A comparison of the performance of children with and without autism on the sensory profile. *American Journal of Occupational Therapy*, *51*(7), 530–537. https://doi.org/10.5014/ajot.51.7.530

Kleiner, M., Brainard, D., Pelli, D., Ingling, A., Murray, R., & Broussard, C. (2007). What's new in psychtoolbox-3. *Perception*, *36*(4), 1–16.

Kriegeskorte, N., Simmons, W. K., Bellgowan, P. S., & Baker, C. I. (2009). Circular analysis in systems neuroscience: The dangers of double dipping. *Nature Neuroscience*, *12*(5), 535–540. https://doi.org/10.1038/nn.2303

Kriss, I., & Evans, B. J. W. (2005). The relationship between dyslexia and Meares-Irlen syndrome. *Journal of Research in Reading*, *28*(3), 350–364. https://doi.org/10.1111/j.1467-9817.2005.00274.x

Lakens, D., Adolfi, F. G., Albers, C. J., Anvari, F., Apps, M. A., Argamon, S. E., Baguley, T., Becker, R. B., Benning, S. D., Bradford, D. E., Buchanan, E. M., Caldwell, A. R., Van Calster, B., Carlsson, R., Chen, S.-C., Chung, B., Colling, L. J., Collins, G. S., Crook, Z., … Zwaan, R. A. (2018). Justify your alpha. *Nature Human Behaviour*, *2*(3), 168–171. https://doi.org/10.1038/s41562-018-0311-x

Lassalle, A., & Itier, R. J. (2013). Fearful, surprised, happy, and angry facial expressions modulate gaze-oriented attention: Behavioural and ERP evidence. *Social Neuroscience*, *8*(6), 583–600. https://doi.org/10.1080/17470919.2013.835750

Lehtonen, J. B. (1974). Visual evoked cortical potentials for single flashes and flickering light in migraine. *Headache: The Journal of Head and Face Pain*, *14*(1), 1–12. https://doi.org/10.1111/j.1526-4610.1974.hed1401001.x

Lorca-Puls, D. L., Gajardo-Vidal, A., White, J., Seghier, M. L., Leff, A. P., Green, D. W., Crinion, J. T., Ludersdorfer, P., Hope, T. M. H., Bowman, H., & Price, C. J. (2018). The impact of sample size on the reproducibility of voxel-based lesion-deficit mappings. *Neuropsychologia*, *115*, 101–111. https://doi.org/10.1016/j.neuropsychologia.2018.03.014

Luck, S. J. (2014). *An Introduction to the Event-Related Potential Technique*. MIT press.

Luck, S. J., Heinze, H. J., Mangun, G. R., & Hillyard, S. A. (1990). Visual event-related potentials index focused attention within bilateral stimulus arrays. II. Functional dissociation of P1 and N1 components. *Electroencephalography and Clinical Neurophysiology*, *75*(6), 528–542. https://doi.org/10.1016/0013-4694(90)90139-B

Luck, S. J., & Hillyard, S. A. (1994). Electrophysiological correlates of feature analysis during visual search. *Psychophysiology*, *31*, 291–308. https://doi.org/10.1111/j.1469-8986.1994.tb02218.x

Luck, S. J., Woodman, G. E., & Vogel, E. K. (2000). Event-related potential studies of attention. *Trends in Cognitive Sciences*, *4*, 432–440. https://doi.org/10.1016/S1364-6613(00)01545-X

MacLean, C., Appenzeller, O., Cordaro, J. T., & Rhodes, J. (1975). Flash evoked potentials in migraine. *Headache: The Journal of*

Head and Face Pain, *14*(4), 193–198. https://doi.org/10.1111/j.1526-4610.1975.hed1404193.x

Mangun, G. R. (1995). Neural mechanisms of visual selective attention. *Psychophysiology*, *32*(1), 4–18. https://doi.org/10.1111/j.1469-8986.1995.tb03400.x

Mangun, G. R., & Hillyard, S. A. (1991). Modulations of sensory-evoked brain potentials indicate changes in perceptual processing during visual-spatial priming. *Journal of Experimental Psychology: Human Perception and Performance*, *17*(4), 1057–1074. https://doi.org/10.1037/0096-1523.17.4.1057

Marks, D. A., & Ehrenberg, B. L. (1993). Migraine-related seizures in adults with epilepsy, with EEG correlation. *Neurology*, *43*(12), 2476–2476, 2483. https://doi.org/10.1212/WNL.43.12.2476

Munte, T. F., Heinze, H. J., & Mangun, G. R. (1995). Luminance and spatial attention effects on early visual processing. *Cognitive Brain Research*, *2*, 189–205.

Muthukumaraswamy, S. D., Evans, C. J., Edden, R. A. E., Wise, R. G., & Singh, K. D. (2012). Individual variability in the shape and amplitude of the BOLD-HRF correlates with endogenous GABAergic inhibition. *Human Brain Mapping*, *33*(2), 455–465. https://doi.org/10.1002/hbm.21223

Ng, B. S. W., Logothetis, N. K., & Kayser, C. (2013). EEG phase patterns reflect the selectivity of neural firing. *Cerebral Cortex*, *23*, 389–398. https://doi.org/10.1093/cercor/bhs031

Nulty, D. D., Wilkins, A. J., & Williams, M. G. (1987). Mood, pattern sensitivity and headache: a longitudinal study. *Psychological Medicine*, *17*, 705–713.

Olman, C. A., Ugurbil, K., Schrater, P., & Kersten, D. (2004). BOLD fMRI and psychophysical measurements of contrast response to broadband images. *Vision Research*, *44*(7), 669–683. https://doi.org/10.1016/j.visres.2003.10.022

Omland, P. M., Nilsen, K. B., Uglem, M., Gravdahl, G., Linde, M., Hagen, K., & Sand, T. (2013). Visual evoked potentials in interictal migraine: No confirmation of abnormal habituation. *Headache: The Journal of Head and Face Pain*, *53*(7), 1071–1086. https://doi.org/10.1111/head.12006

Omland, P. M., Uglem, M., Hagen, K., Linde, M., Tronvik, E., & Sand, T. (2016). Visual evoked potentials in migraine: Is the "neurophysiological hallmark" concept still valid? *Clinical Neurophysiology*, *127*(1), 810–816. https://doi.org/10.1016/j.clinph.2014.12.035

Pelli, D. G. (1997). The VideoToolbox software for visual psychophysics: Transforming numbers into movies. *Spatial Vision*, *10*, 437–442.

Richey, E. T., Kooi, K. A., & Waggoner, R. W. (1966). Visually evoked responses in migraine. *Electroencephalography and Clinical Neurophysiology*, *21*(1), 23–27. https://doi.org/10.1016/0013-4694(66)90055-1

Saksida, A., Iannuzzi, S., Bogliotti, C., Chaix, Y., Démonet, J. F., Bricout, L., Billard, C., Nguyen-Morel, M. A., Le Heuzey, M. F., Soares-Boucaud, I., & George, F. (2016). Phonological skills, visual attention span, and visual stress in developmental dyslexia. *Developmental Psychology*, *52*(10), 1503–1516. https://doi.org/10.1037/dev0000184

Schoenen, J., Wang, W., Albert, A., & Delwaide, P. J. (1995). Potentiation instead of habituation characterizes visual evoked potentials in migraine patients between attacks. *European Journal of Neurology*, *2*(2), 115–122. https://doi.org/10.1111/j.1468-1331.1995.tb00103.x

Schwedt, T. J., Chiang, C. C., Chong, C. D., & Dodick, D. W. (2015). Functional MRI of migraine. *The Lancet Neurology*, *14*(1), 81–91. https://doi.org/10.1016/S1474-4422(14)70193-0

Semyanov, A., Walker, M. C., & Kullmann, M. M. (2003). GABA uptake regulates cortical excitability via cell type–specific tonic inhibition. *Nature Neuroscience*, *6*(5), 484–490. https://doi.org/10.1038/nn1043

Shahaf, G. (2016). Migraine as dysfunctional drive reduction: Insight from electrophysiology. *Medical Hypotheses*, *91*, 62–66. https://doi.org/10.1016/j.mehy.2016.04.017

Shepherd, A. J., & Joly-Mascheroni, R. M. (2017). Visual motion processing in migraine: Enhanced motion after-effects are related to display contrast, visual symptoms, visual triggers and attack frequency. *Cephalalgia*, *37*(4), 315–326. https://doi.org/10.1177/0333102416640519

Shin, Y.-W., Krishnan, G., Hetrick, W. P., Brenner, C. A., Shekhar, A., Malloy, F. W., & O'Donnell, B. F. (2010). Increased temporal variability of auditory event-related potentials in schizophrenia and schizotypal personality disorder. *Schizophrenia Research*, *124*, 110–118. https://doi.org/10.1016/j.schres.2010.08.008

Shirazibeheshti, A., Cooke, J., Chennu, S., Adapa, R., Menon, D. K., Hojjatoleslami, S. A., Witon, A., Li, L., Bekinschtein, T., & Bowman, H. (2018). Placing meta-stable states of consciousness within the predictive coding hierarchy: The deceleration of the accelerated prediction error. *Consciousness and Cognition*, *63*, 123–142. https://doi.org/10.1016/j.concog.2018.06.010

Singleton, C., & Trotter, S. (2005). Visual stress in adults with and without dyslexia. *Journal of Research in Reading*, *28*, 365–378. https://doi.org/10.1111/j.1467-9817.2005.00275.x

Spierings, E. L., Ranke, A. H., & Honkoop, P. C. (2001). Precipitating and aggravating factors of migraine versus tension-type headache. *Headache: The Journal of Head and Face Pain*, *41*(6), 554–558. https://doi.org/10.1046/j.1526-4610.2001.041006554.x

Tanner, D., Morgan-Short, K., & Luck, S. J. (2015). How inappropriate high-pass filters can produce artifactual effects and incorrect conclusions in ERP studies of language and cognition. *Psychophysiology*, *52*(8), 997–1009. https://doi.org/10.1111/psyp.12437

Utama, N. P., Takemoto, A., Koike, Y., & Nakamura, K. (2009). Phased processing of facial emotion: An ERP study. *Neuroscience Research*, *64*(1), 30–40. https://doi.org/10.1016/j.neures.2009.01.009

Van Voorhis, S., & Hillyard, S. A. (1977). Visual evoked potentials and selective attention to points in space. *Perception and Psychophysics*, *22*(1), 54–62.

Vazquez, A. L., & Noll, D. C. (1998). Nonlinear aspects of the BOLD response in functional MRI. *NeuroImage*, *7*(2), 108–118. https://doi.org/10.1006/nimg.1997.0316

Vecchia, D., & Pietrobon, D. (2012). Migraine: A disorder of brain excitatory–inhibitory balance? *Trends in Neurosciences*, *35*(8), 507–520. https://doi.org/10.1016/j.tins.2012.04.007

Vieira, A., Van der Linde, I., Bright, P., & Wilkins, A. (2020). Preference for lighting chromaticity in migraine with aura. *Headache*, *60*, 1124–1131. https://doi.org/10.1111/head.13801

Vogel, E. K., & Luck, S. J. (2000). The visual N1 component as an index of a discrimination process. *Psychophysiology*, *37*(2), 190–203. https://doi.org/10.1111/1469-8986.3720190

Wang, W., Wang, G. P., Ding, X. L., & Wang, Y. H. (1999). Personality and response to repeated visual stimulation in migraine and tension-type headaches. *Cephalalgia*, *19*(8), 718–724. https://doi.org/10.1046/j.1468-2982.1999.019008718.x

Welch, K. M., D'Andrea, G., Tepley, N., Barkley, G., & Ramadan, N. M. (1990). The concept of migraine as a state of central neuronal hyperexcitability. *Neurological Clinics*, *8*(4), 817–828.

Wetzels, R., Matzke, D., Lee, M. D., Rouder, J. N., Iverson, G. J., & Wagenmakers, E. J. (2011). Statistical evidence in experimental psychology: An empirical comparison using 855 t tests. *Perspectives on Psychological Science*, *6*(3), 291–298. https://doi.org/10.1177/1745691611406923

Wilkins, A. (1986). Intermittent illumination from visual display units and fluorescent lighting affects movements of the eyes across text. *Human Factors*, *28*(1), 75–81. https://doi.org/10.1177/001872088602800108

Wilkins, A., Nimmo-Smith, I. A. N., Tait, A., McManus, C., Sala, S. D., Tilley, A., Arnold, K., Barrie, M., & Scott, S. (1984). A neurological basis for visual discomfort. *Brain*, *107*(4), 989–1017. https://doi.org/10.1093/brain/107.4.989

Wilkins, A. J. (1995). *Oxford Psychology Series, No. 24.Visual Stress*. UK: Oxford University Press. Oxford.

Wilkins, A. J. (2003). Reading through colour. In *How Coloured Filters Can Reduce Reading Difficulty, Eye Strain, and Headaches*. NJ: Wiley.

Wilkins, A. J., Allen, P. M., Monger, L., & Gilchrist, J. (2016). Visual stress and dyslexia for the practising optometrist. *Optometry in Practice*, *17*(2), 103–112.

Wilkins, A. J., Binnie, C. D., & Darby, C. E. (1980). Visually-induced seizures. *Progress in Neurobiology*, *15*, 85–117.

Wilkins, A. J., Darby, C. E., & Binnie, C. D. (1979). Neurophysiological aspects of pattern-sensitive epilepsy. *Brain*, *102*(1), 1–25. https://doi.org/10.1093/brain/102.1.1

Wilkins, A. J., & Evans, B. J. W. (2001). *Pattern Glare Test Instructions*. London, UK: IOO Sales Ltd.

Wilkins, A. J., Nimmo-Smith, I., Slater, A. I., & Bedocs, L. (1989). Fluorescent lighting, headaches and eyestrain. *Lighting Research & Technology*, *21*(1), 11–18. https://doi.org/10.1177/096032718902100102

Wright, B. N., Wilkins, A. J., & Zoukos, Y. (2007). Spectral filters can improve reading and visual search in patients with multiple sclerosis. *Journal of Neurology*, *254*(12), 1729–1735. https://doi.org/10.1007/s00415-007-0648-y

Zhang, G. L., Cong, L. J., Song, Y., & Yu, C. (2013). ERP P1-N1 changes associated with Vernier perceptual learning and its location specificity and transfer. *Journal of Vision*, *13*(4), 19–19. https://doi.org/10.1167/13.4.19

SUPPORTING INFORMATION

Additional supporting information may be found in the online version of the article at the publisher's website.

How to cite this article: Tempesta, A. J., Miller, C. E., Litvak, V., Bowman, H., & Schofield, A. J. (2021). The missing N1 or jittered P2: Electrophysiological correlates of pattern glare in the time and frequency domain. *European Journal of Neuroscience*, *54*(6), 6168–6186. https://doi.org/10.1111/ejn.15419